Science of the Total Environment 633 (2018) 341–351

Contents lists available at ScienceDirect

Science of the Total Environment

journal homepage: www.elsevier.com/locate/scitotenv

Exploring synergistic benefits of Water-Food-Energy Nexus through multi-objective reservoir optimization schemes

Tinn-Shuan Uen [a], Fi-John Chang [a,*], Yanlai Zhou [a,b], Wen-Ping Tsai [a]

[a] Department of Bioenvironmental Systems Engineering, National Taiwan University, Taipei 10617, Taiwan, ROC
[b] State Key Laboratory of Water Resources and Hydropower Engineering Science, Wuhan University, Wuhan 430072, China

HIGHLIGHTS

- Propose a holistic scheme to synergistically optimize the benefits of WFE Nexus
- NSGA-II optimizes reservoir operation to maximize hydropower output and impoundment.
- Water supply is simulated by joint operation of the reservoir and irrigation ponds.
- Reduce water shortage rate by 22% & increase hydropower benefit by 9.33 m USD/year
- The proposed methodology is a viable approach to promoting synergistic benefits.

GRAPHICAL ABSTRACT

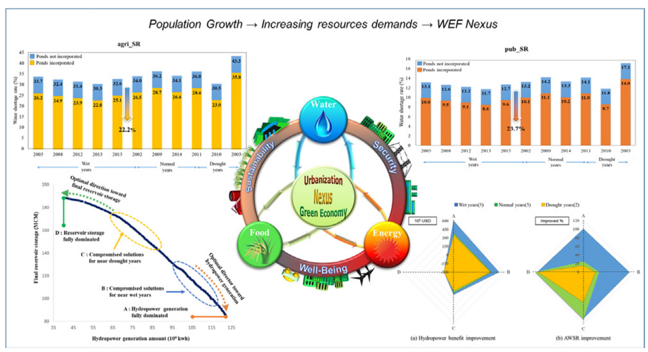

ARTICLE INFO

Article history:
Received 7 December 2017
Received in revised form 14 March 2018
Accepted 16 March 2018
Available online xxxx

Editor: Simon Pollard

Keywords:
Water-Food-Energy Nexus
Multi-objective optimization
Synergistic benefits
Artificial intelligence (AI)
NSGA-II

ABSTRACT

This study proposed a holistic three-fold scheme that synergistically optimizes the benefits of the Water-Food-Energy (WFE) Nexus by integrating the short/long-term joint operation of a multi-objective reservoir with irrigation ponds in response to urbanization. The three-fold scheme was implemented step by step: (1) optimizing short-term (daily scale) reservoir operation for maximizing hydropower output and final reservoir storage during typhoon seasons; (2) simulating long-term (ten-day scale) water shortage rates in consideration of the availability of irrigation ponds for both agricultural and public sectors during non-typhoon seasons; and (3) promoting the synergistic benefits of the WFE Nexus in a year-round perspective by integrating the short-term optimization and long-term simulation of reservoir operations. The pivotal Shihmen Reservoir and 745 irrigation ponds located in Taoyuan City of Taiwan together with the surrounding urban areas formed the study case. The results indicated that the optimal short-term reservoir operation obtained from the non-dominated sorting genetic algorithm II (NSGA-II) could largely increase hydropower output but just slightly affected water supply. The simulation results of the reservoir coupled with irrigation ponds indicated that such joint operation could significantly reduce agricultural and public water shortage rates by 22.2% and 23.7% in average, respectively, as compared to those of reservoir operation excluding irrigation ponds. The results of year-round short/long-term joint operation showed that water shortage rates could be reduced by 10% at most, the food production rate could be increased by up to 47%, and the hydropower benefit could increase up to 9.33 million USD per year, respectively, in a wet year. Consequently, the proposed methodology could be a viable approach to promoting the synergistic benefits of the WFE Nexus, and the results provided unique insights for stakeholders and policymakers to pursue sustainable urban development plans.

* Corresponding author.
E-mail address: changfj@ntu.edu.tw (F.-J. Chang).

https://doi.org/10.1016/j.scitotenv.2018.03.172
0048-9697/

1. Introduction

The Water, Food and Energy (WFE) Nexus has gained increasing attention globally in research, business and policy spheres whose developments have been highly interlinked by joint demands and resource constraints. The WFE Nexus is a newest integrated management paradigm in environmental sciences (Al-Saidi and Elagib, 2017; Wichelns, 2017; Weitz et al., 2017). The interactions between WFE sectors undoubtedly attract paramount interest of policy, science and society domains, today and even more interest in the upcoming decades, as we are facing the great challenges of population increase, food shortage, water scarcity and energy resources insufficiency in many parts of the world. These interdependencies and effects are further influenced by trade, markets and speculations, as seen in the joint price movements of energy and agricultural products (Ringler et al., 2013; Bieber et al., 2018; Scanlon et al., 2017; Tarroja et al., 2014). As a result of greenhouse gas emission control, the WFE production and delivery may also raise impacts on environments (Zhang and Vesselinov, 2017). The global environmental changes and urbanization further complicate the WFE Nexus challenges and make the interrelationship between these sectors highly dynamic. Without adequate mechanisms for transporting or exchanging WFE nutrients from production areas (rural or peri-urban) to urban areas, the possibility to achieve urban sustainability would be questioned. Thus it is a great challenge to pursue sustainable urban development under growing population and increasing living standards with limited WFE resources (Cosgrove and Loucks, 2015; Machell et al., 2015; Vilanova and Balestieri, 2015; Y. Chang et al., 2016; Garcia and You, 2016; Smajgl et al., 2016; Barik et al., 2017; Pereira, 2017). Despite the concept of the WFE Nexus that has emerged as a useful way to analyze the complex and interrelated pressures on the three main global resource systems, little effort has been made to explore the nexus perspective for optimizing WFE-related synergistic benefits ever since (Rasul and Sharma, 2016; Bieber et al., 2018).

WFE sectors have inherent nexus, and the development of one sector usually consumes resources in the other two sectors. Due to existing institutional structures (e.g., different governmental bureaus manage water, food and energy, respectively), insufficient administrative coordination usually occurs when making important planning and decisions on WFE. Policymakers and stakeholders may fail to consider sustainability challenges in a holistic way or ignore the nexus among WFE sectors. We notice that the number of studies focusing on modeling WFE Nexus in water resources management, energy production, urban design and policy analysis through various techniques, such as life cycle assessment (Ali and Kumar, 2017), carbon footprint (Miller and Carriveau, 2017), water footprint (Chini et al., 2017; Hoekstra, 2017), supply chain management (Allan et al., 2015; Owen et al., 2018), system dynamic (El-Gafy, 2014; Feng et al., 2016) and multi-objective reservoir operation (Zhou et al., 2015; De et al., 2016; Jalilov et al., 2016), have dramatically increased in the last few years. Among them, multi-objective reservoir operation implemented by optimization techniques is one of the most promising methods for improving synergistic benefits of the WFE Nexus (Castelletti et al., 2012; Ramos et al., 2013; Ahmad et al., 2014; Hurford and Harou, 2014; Bai et al., 2015; Chu et al., 2015).

Taiwan has subtropical weather and mountainous topography such that each hydrological year can be segmented into seasonally dry and wet periods by typhoon seasons, where typhoons commonly bring heavy rainfall, around 600–1000 mm in just a few days, and thus cause highly variable river flow. Reservoir operation can play a key role in synergistically optimizing the benefits of the WFE Nexus for solving such river flow variability and improving water availability, flood control, hydropower generation and other services. Vörösmarty et al. (2010) provided a nice illustration of how dams were part of the WEF Nexus, and Jalilov et al. (2016) applied two potential operation modes, i.e. energy mode (hydropower) and irrigation mode (agriculture), to the dam for managing the WFE Nexus. Rapidly growing water demands under limited water supply put high pressure on water-intensive energy and food production, and therefore alternative approaches are desired, particularly for areas like Taipei metropolitan area with large inter-sectoral competition for water. Previous applications of reservoir operation aimed at improving benefits from either short-term flood control operation or long-term water supply operation (e.g., Chang and Chang, 2009; Chou and Wu, 2015; Hsu et al., 2015; Tsai et al., 2015; F.J. Chang 2016). However, to the best of our knowledge, the study of optimal synergistic benefits of the WFE Nexus on the basis of joint reservoir operation is rare. Bearing this in mind as a motivation, this study intended to model short/long-term joint operation for a multi-objective reservoir so as to optimize the balance between hydropower generation and reservoir impoundment during flood seasons and to improve the synergistic benefits of the WFE Nexus in a year-round perspective. The Shihmen Reservoir, 745 irrigation ponds (considered as a virtual reservoir for joint reservoir operation purpose) and multiple water users in northern Taiwan formed a case study.

This study comprised three major parts: (1) obtaining the optimal short-term reservoir operation strategy from the trade-off between hydropower generation and final reservoir storage during typhoon seasons by using optimization techniques; (2) estimating the long-term water shortage rates of agricultural and public water sectors based on reservoir rule curves and irrigation pond-water availability simulation during non-typhoon seasons; and (3) improving the synergistic benefits of the WFE Nexus by integrating the optimization of short-term reservoir operation with the simulation of long-term reservoir operation in a year-round perspective. This study seeked to increase the understanding of the interlinkages within the WFE Nexus and considered this nexus in the context of adaptation responses that improve resource use efficiency and encourage multi-sectoral policy deliberation and coherence. This paper is organized as follows. Section 2 briefly introduces the study area and data collection. Section 3 describes the methodology adopted in this study. The results and discussion are shown in Section 4, and final remarks are drawn in Section 5.

2. Study area and data collection

2.1. Study area

The Shihmen Reservoir, a multi-purpose reservoir located in Taoyuan City, Taiwan, is the pivotal reservoir for the Taipei metropolitan area while its effective storage capacity reaches 201 million m^3 and its watershed area occupies 763 km^2. The crest of the dam is at an elevation of 252.1 m, the top of the flood control pool is at an elevation of 250 m, the normal maximum water level of the conservation pool is at 245 m, and the dead water level is at 195 m. Besides, each of the six floodgates of the ogee-type concrete spillway is of 14 m × 10.61 m with minimum discharge of 600 m^3/s and maximum discharge up to 11,400 m^3/s. There also exist two tunnel spillways with a minimum discharge of 200 m3/s and maximum discharge 2400 m3/s (Chang, 2008). The mainstream in this catchment is the Tamsui River, which has a length of about 159 km in total and a drainage area of about 2726 km^2. Fig. 1 shows the distribution diagram of the water supply system and the Shihmen Reservoir Watershed. The water distribution area covers the Tamsui River Basin and other small river basins, in which the Shihmen and Taoyuan irrigation areas occupy 121 km^2 and 270 km^2, respectively. The multi-purpose of the Shihmen Reservoir includes water supply (public and agricultural sectors), hydropower generation and flood control. The average annual rainfall in this watershed is about 2500 mm, and the main flood season in response to typhoon invasion starts from July to September. The water supply target of the Shihmen Reservoir in early stage was irrigation sectors, but it was gradually shifted to public (domestic and industrial) and agricultural sectors as the fast development of urbanization occurred in the Taipei metropolitan area in the last three decades. Serving as a multi-objective reservoir with limited storage capacity under highly uncertain hydrological conditions, it is a very complicated

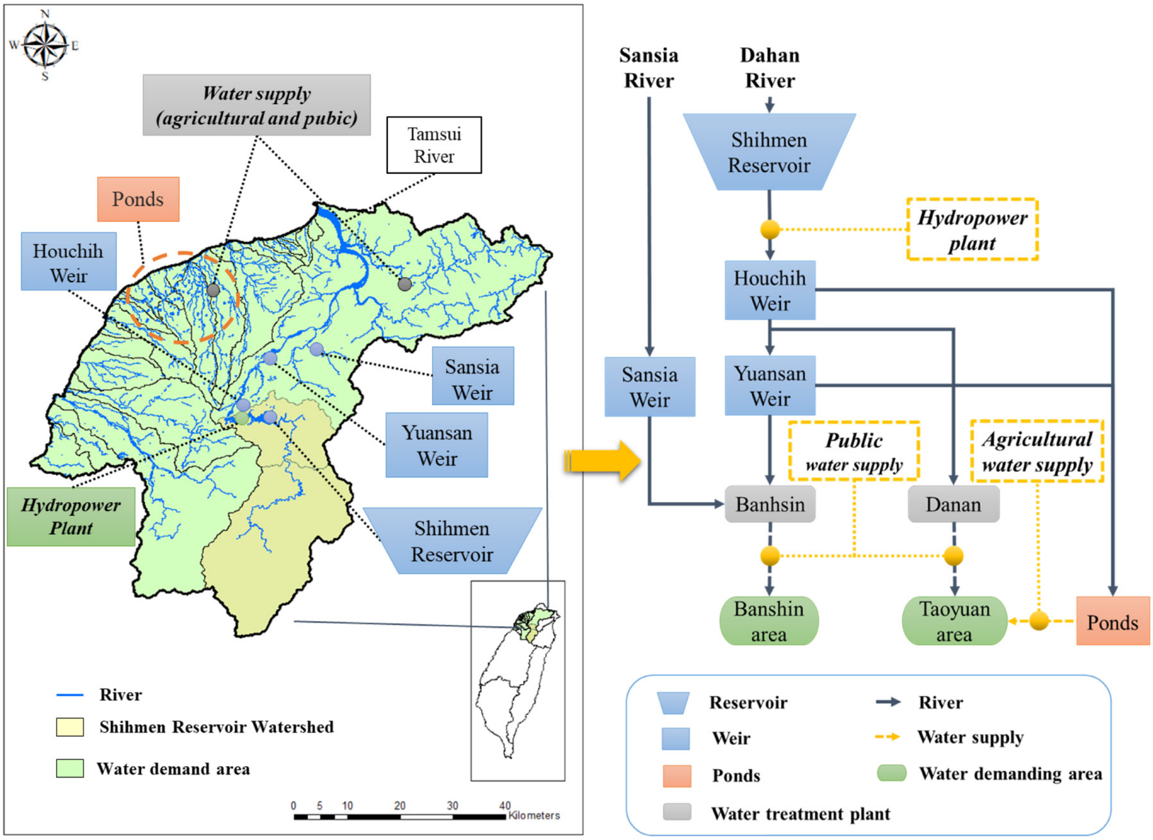

Fig. 1. Distribution diagram of the water supply system and the Shihmen Reservoir watershed.

and challenging task to systematically consider both the safety of short-term reservoir operation and the reliability of long-term water supply to multi-sectors. Besides, a great number (745) of irrigation ponds, with a total capacity of about 62 million m^3, spread over Taoyuan City, which could be considered as another irrigation water source, especially for drought periods.

When the conflicts between different water demands occur, the Official Operative Regulation (M-5 rule curves) of the Shihmen Reservoir is adopted to guide reservoir operation, as shown in Fig. 2. The M-5 rule curves can help administrators to adjust the strategies made for water reallocation under different circumstances. The M-5 rule curves contains three curves, i.e. upper limit, lower limit and critical limit. At present, the priority of water supply is given in the sequence of public sectors, agricultural sectors and hydropower generation. The corresponding regulations are: (1) when the reservoir water level exceeds the upper limit, water supply will satisfy the planned water demands and can be increased if necessary; (2) when the water level falls between the upper and lower limits, the water supply can still satisfy the planned water demands; (3) when the water level falls between the lower and critical limits, the water supply can provide 75% and 90% of the planned water demands for agricultural and public sectors, respectively; and (4) when the water level falls below the critical

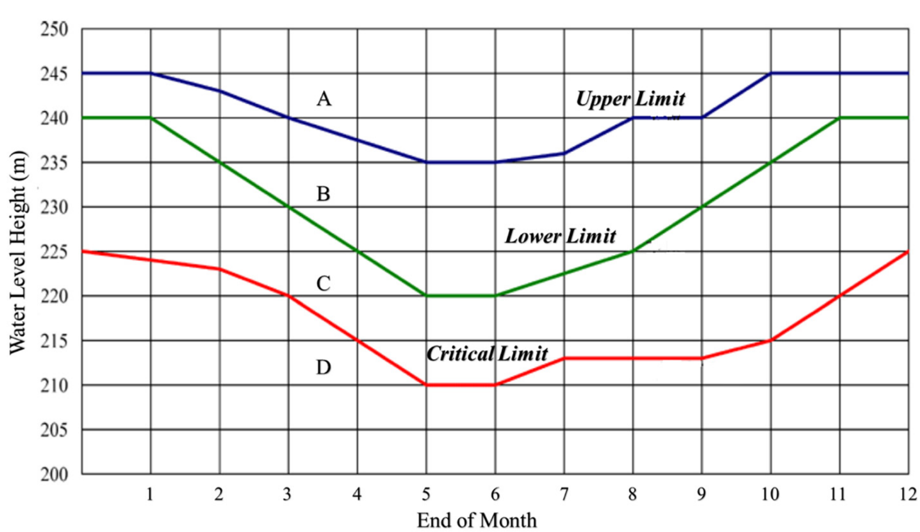

Fig. 2. Official Operative Regulation of the Shihmen Reservoir (M-5 rule curves).

limit, the water supply can only provide 50% and 80% of the planned water demands for agricultural and public sectors, respectively.

2.2. Data collection

The data used for modeling both long-term and short-term reservoir operation consisted of the initial reservoir storage and total reservoir inflow of the Shihmen Reservoir, public water demand, agricultural water demand, and the total availability of 745 irrigation ponds in Taoyuan City, which were collected during 2002–2015 (Table 1). Data applied to the optimization of short-term (daily scale) reservoir operations consisted of 1196 datasets [=11 (inflow scenarios) ∗ 92 (days, from July to September) + 2 (agricultural and public water demands) ∗ 92] while data applied to the simulation of long-term (ten-day scale) reservoir operations consisted of 162 datasets [=2 (inflow scenarios) ∗ 27 (10-day periods, from October to June) ∗ 3 (water demands)].

3. Methodology

In this study, the core methodology contained two parts: optimization of short-term (daily scale) reservoir operation during typhoon seasons (July–October) and simulation of long-term (ten-day scale) reservoir operation during non-typhoon seasons (November–the next June). For the short-term stage, we improved reservoir operation for maximizing hydropower output and the reservoir storage at the end of the typhoon season by using an optimization technique. For the long-term stage, we considered the optimal results of the final reservoir storage obtained from short-term reservoir operation as the input (initial reservoir storage) of long-term reservoir operation during non-typhoon seasons, and then conducted water allocation simulation based on the joint operation of the reservoir and irrigation ponds under the scenarios of drought years for achieving the year-round reservoir operation, in view of a hydrological year (July-the next June). The overall framework of short/long-term reservoir operation implemented in this study is shown in Fig. 3.

The Non-dominated sorting genetic algorithm II (NSGA-II) was used to optimize the short-term multi-objective daily reservoir operations under thirty scenarios (i.e. ten reservoir inflows with three initial water levels). We then conduct M-5 rule curves to simulate reservoir operation during non-typhoon seasons for evaluating the feasibility of hydropower generation and security of water supply for the reservoir. We utilized the most drought situations in the past two decades as the reservoir inflows (inputs) of the simulation model at a time scale of ten days and then adopted current (2017) water demands to calculate the water shortage rates of public (domestic and industrial) and agricultural sectors. Moreover, we explored the improvement of water deficit by incorporating the water supply from a virtual reservoir (a union of 745 irrigation ponds scattered over the Taoyuan irrigation area, considered as a backup for the Shihmen Reservoir). Ultimately, we integrated short-term and long-term reservoir operations into a year-round analysis to explore the reliability of future water supply and summarized the outputs of all optimal solutions for the WFE Nexus to analyze the overall synergistic benefits. The brief introduction of the methods adopted is given as follows.

Table 1
Statistics of the data collected from the investigative area during 2002 and 2015.

Data type (MCM[a])	Typhoon season[b]	Non-typhoon season[c]	Average annual value
Reservoir[d] storage	201	201	201
Total inflow	[338, 1108, 1504][e]	[823, 1324, 1984]	1526
Public water demand[c]	[58, 104, 130]	[188, 305, 419]	447
Agricultural water demand[c]	[153, 159, 163]	[327, 331, 338]	484
Total capacity of 745 irrigation ponds	62.38	62.38	62.38

[a] Million cubic meters.
[b] Daily scale starting from July to September.
[c] Ten-day scale starting from October to the June.
[d] The reservoir watershed area occupies 763 km^2, and the water demand area shown in Fig. 1 covers about 3800 km^2.
[e] [minimum, mean, maximum].

3.1. Optimization of short-term multi-objective reservoir operation by using the NSGA-II

3.1.1. Non-dominated sorting genetic algorithm II (NSGA-II)

The NSGA-II, proposed by Deb et al. (2002), was improved from the genetic algorithm (GA) (Deb et al., 2000) and was widely used in solving various water resources management issues (e.g., Chang and Chang, 2009; Haghighi and Asl, 2014; Tabari and Soltani, 2013; Tsai et al., 2015; Zhou et al., 2015). The main operators contain the reproduction, mating, and mutation ones of the GA together with the non-dominated sorting and the crowding distance sorting ones. By searching parental and offspring generations, this searching mechanism not only retains a large number of good solutions from parents but also increase the diversity of solutions. Also, the non-dominated sorting operator improves the searching efficiency with the elite strategy. The results obtained from the NSGA-II will generally form the Pareto Front solutions, which offer a variety of optimal strategies to decision makers and stakeholders.

The implementation of the NSGA-II in this study adopts the following procedure.

Step 1: Initialize a population P_0 of size N randomly and evaluate their fitness values; partition the population into different ranks through the fast non-dominated sorting; and calculate the crowding distances of the population according to Eq. (1).

$$C_{M,i} = \begin{cases} \infty & \text{if } f_{M,i} = \max(f_M) \text{ or } \min(f_M) \\ \dfrac{f_{M,i+1} - f_{M,i-1}}{\max(f_M) - \min(f_M)}, & \text{else} \end{cases} \quad (1)$$

where $C_{M,\,i}$ is the crowding distance of the *M*th objection function in the *i*th chromosome; f_M is the *M*th objection function; and $f_{M,\,i}$ is the *M*th objection function in the *i*th chromosome.

Step 2: Implement a binary tournament selection, crossover and polynomial mutation operators to generate an offspring population S_0 of size N.

Step 3: Evaluate the fitness values of S_t for every generation *t*; integrate S_{t-1} and S_t into an intermediate population P_t of size 2N; and partition this integrated population into different ranks and calculate their crowding distances.

Step 4: Choose a new parent population P_{t+1} of size N from P_t using a binary tournament selection; generate an offspring population P_{t+1} through crossover and mutation operators; and evaluate their fitness values.

Step 5: Repeat Steps 3 and 4 until reaching the stop criterion.

To compare the optimized reservoir operation with the original one, this study collected historical reservoir operation data corresponding to selected drought years (no or few typhoons), normal years and wet years (many typhoons) during 2002 and 2015. The initial reservoir water level was set under three scenarios (i.e., 240, 235 and 230 m, respectively), and the water demand was set as the average of the last two years (i.e., 2015 and 2016). We applied the NSGA-II to searching the optimal reservoir operations for maximizing both hydropower output and the final reservoir storage during typhoon seasons, in which the population size was set as 400, the number of iterations was also set as 400, the

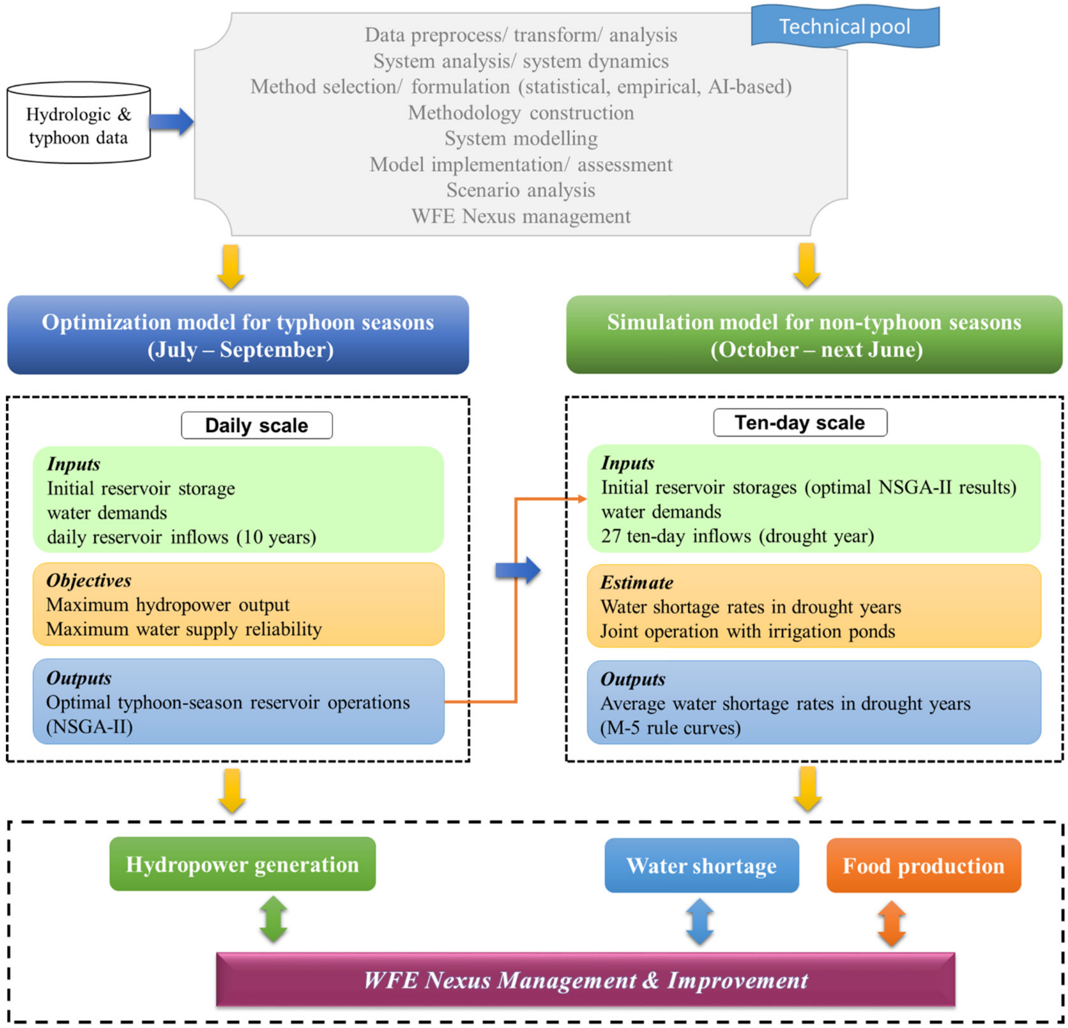

Fig. 3. Framework of optimized short-long-term reservoir operation.

crossover rate was set as 0.8, and the mutation rate was set as 0.1. It was noted that the above parameter setting was obtained from a trial-and-error procedure implemented intensively on the NSGA-II for getting converged results.

3.1.2. Objective functions and constraints

During typhoon seasons, hydropower output and the final reservoir impoundment were selected as the primary objectives. The objective function of hydropower generation was derived from the difference between the reservoir water level and the height of the power tailgate, as shown in the following formula.

Objective function of hydropower generation:

$$\max \sum_{i=1}^{m}\sum_{j=1}^{n} P_{ij}, P_{ij} = kPQ_{ij}\cdot\rho\cdot nctWL_{ij}-h)\cdot t\cdot c^{-1} \quad (2)$$

where P_{ij} denotes the hydropower output (kW·h) for the jth day in the ith year, k denotes the energy conversion efficiency coefficient (set as 0.9), Q_{ij} denotes hydropower outflow (m^3/s) for the jth day in the ith year, ρ is density of water (set as 1000 kg/m^3), g indicates gravitational acceleration (m/s^2), WL_{ij} indicates the height of the reservoir water level (m), h is the height of the power tailgate (set as 125.82 m), t is the number of seconds per day, m denotes the total number of years, n is the total number of operation days (92 days in this study), and c is the conversion factor from Joules (J) to kW·h.

The second objective function was the summation of the final reservoir storages of the selected years, as shown below.

$$\max \sum_{i=1}^{m} S_{i,final} \quad (3)$$

where $S_{i,\ final}$ is the final reservoir storage at the end of the typhoon season in the ith year, and m denotes the total number of selected years. As the reservoir operation is implemented, the safety, operation regulations and physical restrictions of the reservoir need to be contemplated, and the optimal reservoir operations also necessarily obey all the constraints, such as water balance, effective reservoir storage, and discharge limitation.

The mathematical equations for these constraints are presented as follows.

Constraints:

$$S_{j+1} = S_j + (I_j - O1_j - O2_j - O3_j)\cdot\Delta j \quad (4)$$

$$0 \le S_j \le S_{max} \quad (5)$$

$$0 \le O1_j \le O1_{max} \quad (6)$$

$$0 \le S_j, I_j, O1_j, O2_j, O3_j \quad (7)$$

where S_j is the reservoir storage on the jth day, I_j indicates the inflow of the reservoir on the jth day, $O1_j$ is the outflow of hydropower generation on the jth day, $O2_j$ is the spilled water on the jth day, $O3_j$ is the outflow for drainage purpose (irrigation ponds) on the jth day, Δj is the time step (number of seconds per day) on the jth day, S_{max} is the maximum effective reservoir storage, and $O1_{max}$ is the upper limit of outflow for hydropower generation. Eq. (4) represents the mass balance formulation. Eq. (5) indicates the restrictions on reservoir storage capacity. Eq. (6) shows the constraint of water discharge for hydropower generation. Eq. (7) shows the conditional constraints of particular variables, and the time step j ranges from 1 to 92 for all parameters (92 days corresponding to July–September in this study).

3.2. Simulation of long-term water shortage rates coupled with irrigation pond availability

3.2.1. Water shortage rates converted from water supply simulation by using M-5 rule curves

This study analyzed the annual inflow of the Shihmen Reservoir in the past 20 years, as shown in Fig. 4. We noticed that 2002–2003 and 2010–2011 were two driest periods during 1996 and 2015. As a result, we chose those two driest periods as the scenarios for conducting the long-term simulation of water shortage rates. The water demand was adopted as the average of those in 2015 and 2016 for representing the current situation (2017). Finally, nine reservoir water levels (236, 237, 238, … and 244 m) were selected as the initial conditions of the reservoir storage, which were all higher than the upper limit (235 m) of the M-5 rule curves in June (Fig. 2). Following the Official Operation Regulation of the Shihmen Reservoir, we used these designed conditions coupled with observed reservoir inflow to simulate reservoir operation (water supply) for calculating the average water shortage rate (SR) per ten-day period.

The mathematical formulations for the allocation of the water supply system are shown as follows.

$$S'_{k+1} = S'_k + (I'_k - Q'_k) \cdot \Delta k \tag{8}$$

$$Q'_k = SA_k + SP_k - QS_k \tag{9}$$

where S'_k, I'_k and Q'_k are the reservoir storage, reservoir inflow and total reservoir outflow in the kth ten-day period, respectively; and Δk is the time step (the number of seconds per ten-day period). Eq. (8) shows the mass balance formulation. SA_k, SP_k and QS_k are the agricultural water supply, public water supply and spilled water in the kth ten-day period, respectively. Eq. (9) shows the summation of water supply to different users.

The mathematical settings under the operation regulation are shown as follows.

If $S'_k \geq S_{UL}$

$$SA_k \geq DA_k \tag{10}$$

$$SP_k \geq DP_k \tag{11}$$

where S_{UL} is the reservoir storage corresponding to the upper limit of M-5 rule curves. SA_k, DA_k, SP_k and DP_k denote the agricultural water supply, the agricultural water demand, the public water supply and the public water demand in the kth ten-day period, respectively. Eqs. (10) and (11) indicate that water supply must satisfy water demand for both sectors if the reservoir storage is higher than the upper limit S_{UL}.

If $S_{UL} \geq S'_k \geq S_{LL}$

$$SA_k \leq DA_k \tag{12}$$

$$SP_k \leq DP_k \tag{13}$$

where S_{LL} is the reservoir storage corresponding to the lower limit of M-5 rule curves. Eqs. (12) and (13) indicate that water supply will not exceed water demand if the reservoir storage falls between the upper limit S_{UL} and lower limit S_{LL}.

If $S_{LL} \geq S'_k \geq S_{CL}$

$$SA_k = DA_k \cdot 0.75 \tag{14}$$

$$SP_k = DP_k \cdot 0.9 \tag{15}$$

where S_{CL} is the reservoir storage corresponding to the critical limit of M-5 rule curves. Eqs. (14) and (15) indicate that water supply satisfies 75% and 90% of water demands in agricultural and public sectors, respectively, if the reservoir storage falls between the lower limit S_{LL} and critical limit S_{CL}.

If $S_{CL} \geq S'_k$

$$SA_k = DA_k \cdot 0.5 \tag{16}$$

$$SP_k = DP_k \cdot 0.8 \tag{17}$$

Eqs. (16) and (17) indicate that water supply satisfies 50% and 80% of water demands in agricultural and public sectors, respectively, if the reservoir storage is lower than the critical limit S_{CL}. When the

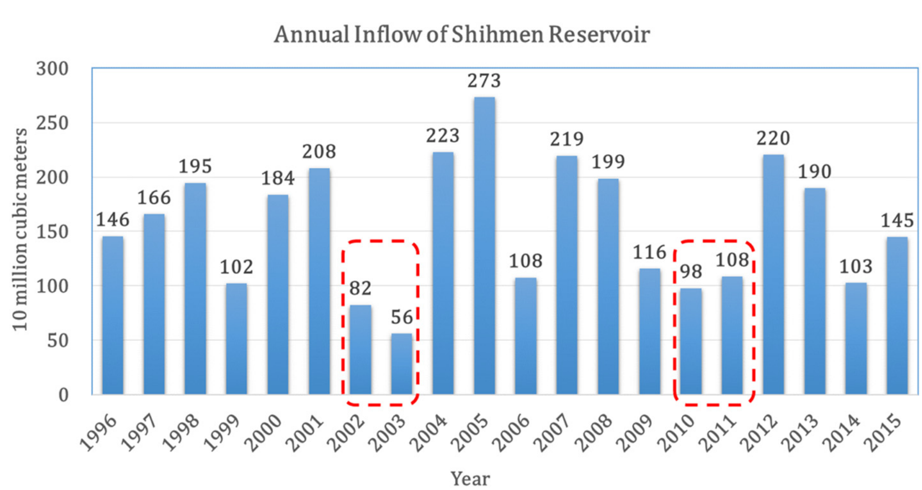

Fig. 4. Annual inflow of the Shihmen Reservoir during1996 and 2015.

water supply is less than the planned water demand, it will induce water shortage problems. The related calculations are shown as follows.

$$DFA_k = (DA_k - SA_k) \cdot \Delta k \quad (18)$$

$$DFP_k = (DP_k - SP_k) \cdot \Delta k \quad (19)$$

$$agri\_SR_k = (DFA_k / DA_k) \quad (20)$$

$$pub\_SR_k = (DFP_k / DP_k) \quad (21)$$

where DFA_k and DFP_k denote agricultural and public water shortages in the kth ten-day period, respectively. Eqs. (18) and (19) shows the differences between water supply and demand in agricultural and public sectors, respectively. $agri\_SR_k$ and pub_SR_k are the agricultural and public water shortage rates shown in Eqs. (20) and (21), respectively. Water loss was ignored in this study.

The relevant constraints are shown as follows.

Constraints

$$0 \le S\prime_k \le S_{max} \quad (22)$$

$$Q\prime_k \le S\prime_k \quad (23)$$

$$0 \le S\prime_k, I\prime_k, Q\prime_k, SA_k, SP_k, QS_k, DFA_k, DFP_k \quad (24)$$

Eq. (22) shows the restriction on reservoir capacity, and Eq. (23) shows the limitation of total reservoir outflow. Eq. (24) shows the conditional constraints for all variables.

3.2.2. Derive water shortage rates from water supply simulation in consideration of irrigation ponds

A great number of irrigation ponds distributed in Taoyuan City were applied to furnishing unsatisfied water demands in this study. The total capacity of all 745 irrigation ponds occupied about 62 million m^3, which was approximately 25% of the storage capacity of the Shihmen Reservoir. It could be expected that the water deficit situations in drought years could be significantly mitigated for both agricultural and public sectors when integrating these irrigation ponds with the reservoir for joint water supply. We set two assumptions for all the irrigation ponds: first, consolidating all 745 irrigation ponds as a virtual reservoir; and second, the initial storage of each pond was full. The reason for assuming a full capacity of the initial pond storage was that the simulation for long-term reservoir operation started from the end of typhoon seasons and we set the amount of water discharge from hydropower generation exceeded the planned water demand such that the excess discharge would flow into irrigation ponds. As a result, the ponds could be easily fulfilled during the entire typhoon seasons.

The formulation of the virtual reservoir (745 irrigation ponds) operation is shown in the following equations.

Virtual reservoir operation:

$$\text{If } SA_k = DA_k \cdot X_k \quad (25)$$

$$PSA_k = DA_k \cdot (1 - X_k) \quad (26)$$

$$\text{else } SA_k = 0 \quad (27)$$

$$PS_{k+1} = PS_k - PSA_k \quad (28)$$

where PS_k is the total effective capacity of all irrigation ponds in the kth ten-day period, PSA_k, DA_k and SA_k denote the water supply of the virtual reservoir, the agricultural water demand and the agricultural water supply in the kth ten-day period, respectively. The M-5 operating rules take into account the agricultural water supply discount rate (X_k) for the first ten-day period of the Shihmen Reservoir operation. Eqs. (25), (26) and (27) show the water supply of the virtual reservoir and the deficit between water supply and demand if a water shortage situation occurs. Eq. (28) shows the water balance equation of the virtual reservoir.

The constraints for the virtual reservoir are shown below.

$$0 \le X_k \le 1 \quad (29)$$

$$PSA_k \le PS_k \quad (30)$$

$$0 \le PSA_k, PS_k, DA_k, SA_k \quad (31)$$

Eq. (29) shows the rationality of the agricultural water supply discount rate, Eq. (30) shows the limitation of irrigation pond water supply, and Eq. (31) shows the conditional constraints for all variables.

4. Results and discussion

The key parts of this study focused on: (1) typhoon seasons – optimizing hydropower output and final reservoir storage by using the NSGA-II; (2) non-typhoon seasons – simulating agricultural and public water shortage rates based on M-5 rule curves in consideration of irrigation pond-water availability; and (3) hydrological year-round perspective – improving the synergistic benefits of the WFE Nexus by integrating the optimal short-term reservoir operation with the simulated long-term reservoir operation. The results are discussed in details, as shown below.

4.1. Optimal short-term reservoir operations during typhoon seasons

In this study, we first aimed at optimizing reservoir operation during typhoon seasons in terms of hydropower generation and final reservoir storage by using the NSGA-II. Fig. 5 presents the 400 Pareto Front solutions of the NSGA-II model under various hydrological scenarios (11 typhoon seasons) during 2002 and 2015. The 400 solutions were uniformly distributed along the Pareto Front with respect to two objectives (power generation and final reservoir storage), where Point A represented the optimal reservoir operation solely considered hydropower generation, while Point D indicated the optimal reservoir operation entirely considered the final reservoir storage. Optimal solutions closer to Point A (e.g., Group B) were more prone to maximizing hydropower output, which indicated the corresponding reservoir operations might be more suitable to implement in wet years (high initial reservoir storages). In contrast, optimal solutions closer to Point D (e.g., Group C) tended to maximize the final reservoir storage but sacrificed hydropower output, which indicated the corresponding reservoir operations

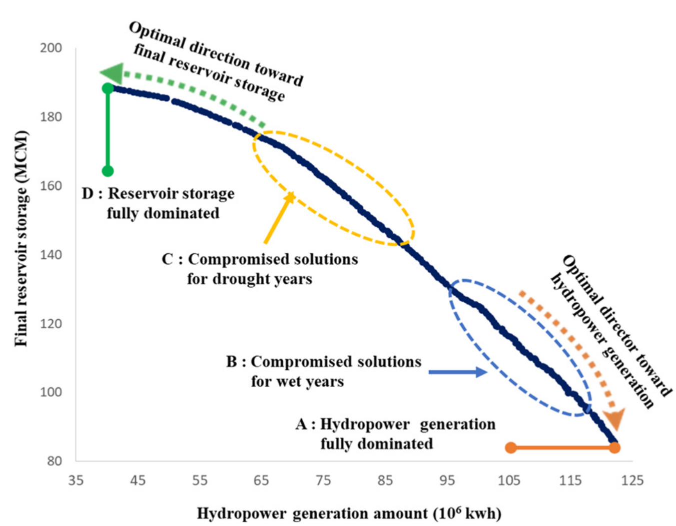

Fig. 5. Pareto Front of the NSGA-II model for long-term reservoir operation of 11 typhoon seasons during 2002 and 2015.

might be more suitable to implement in drought years (low initial reservoir storages).

Table 2 presents three optimal solutions selected from the Pareto front set for representing wet, normal and drought years, respectively. Apparently, the hydropower outputs among the three hydrological conditions varied incredibly, where the mean value of five wet years was four times more than that of two drought years. The final reservoir storage decreased as the reservoir inflow diminished. The lowest final reservoir storage was 139 MCM while the minimum hydropower output was 39 million kW·h in a drought year, which was obtained from the most conservative reservoir operation. In contrast, the final reservoir storage could reach 201 MCM while the hydropower output was 140 million kW·h in a wet year, which did bring a great benefit to both energy and water supply aspects.

4.2. Long-term reservoir operation simulation under various scenarios during non-typhoon seasons

Based on the M-5 rule curves, the water shortage rates for agricultural and public sectors under the scenarios of nine initial reservoir storages were calculated through the simulation of long-term (ten-day scale) reservoir operation. The results were shown in Fig. 6 and Table 3. Fig. 6 shows the results of the simple linear relations of the initial reservoir storage with the water shortage rates in agricultural (agri_SR) and public (pub_SR) sectors in (a) 2002 (drought year) and (b) 2010 (wet year), respectively. The R^2 correlation coefficients of the two regression lines were over 0.94 in the drought year (Fig. 5(a)) and over 0.96 in the wet year (Fig. 5(b)), respectively, which indicated water shortage rates could be highly affected by initial reservoir storages in both wet and drought years. We noticed that both agricultural and public water shortage rates (falling between 10% and 40%) in the drought year (2002) were much higher than those (falling between 0% and 5%) of the wet year (2010), which implied water shortages would be more sensitive to initial reservoir storages in drought years than in wet years. Besides, the agricultural water shortage rates could be significantly mitigated as the initial reservoir storage increased.

Table 3 presents the comparison results between historical reservoir operations and reservoir operation simulations, whose initial reservoir storages were the final reservoir storages optimized by the NSGA-II, in two wet years (2005 and 2013), respectively. It appeared that the optimal reservoir operations produced superior performance than historical ones when maximizing both hydropower output during typhoon seasons and the final reservoir storage during non-typhoon seasons. Besides, the hydropower output almost achieved the maximum capacity of hydropower generators at the final stage and was two times more than that of historical operations, which illustrated the great potential for hydropower output optimization in wet years. For normal and drought years, we noticed that the benefits would be largely decreased during non-typhoon seasons; nevertheless, reservoir operations combined with the optimal NSGA-II results regarding hydropower generation and the final reservoir storage were still more efficient than those of historical operations.

Table 2
Optimal reservoir operations of 11 typhoon seasons during 2002 and 2015 by using the NSGA-II.

Data type	Wet year (5[a])	Normal year (3)	Drought year (2)
Total reservoir inflow (MCM)	[936, 1172, 504][e]	[423, 482, 538]	[314, 286, 338]
IRS[b] (MCM)	161	161	161
HPO[c] (10^6 kWh)	[130, 136, 140]	[69, 74, 76]	[39, 41, 42]
FRS[d] (MCM)	[192, 199, 201]	[168, 182, 196]	[139, 154, 168]

[a] Number of hydrological years.
[b] Initial reservoir storage in July.
[c] Hydropower output.
[d] Final reservoir storage in September.
[e] [minimum, mean, maximum].

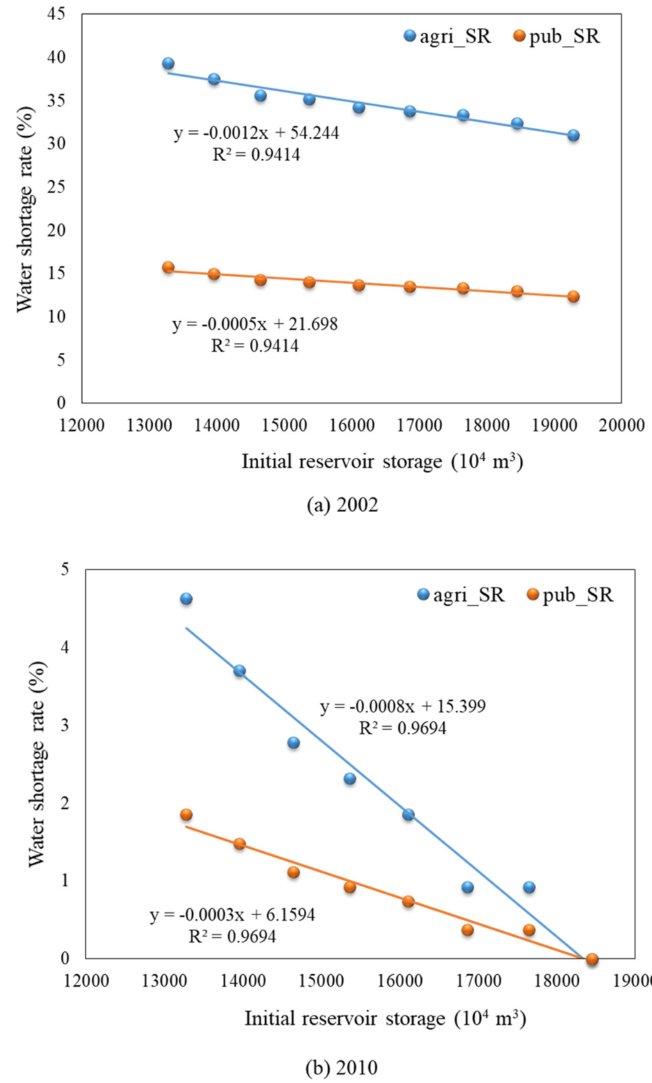

Fig. 6. Linear regression results of the initial reservoir storage corresponding to agricultural and public water shortage rates in (a) 2002 (drought year) and (b) 2010 (wet year), respectively.

4.3. Estimating synergistic benefits of the WFE Nexus

To estimate the synergistic benefits of the WFE Nexus, we combined the optimal short-term reservoir operation with long-term reservoir operation simulation in a year-round perspective. In addition, an incorporation 745 irrigation ponds (virtual reservoir) into the Shihmen Reservoir also implemented to assess the effectiveness of such joint

Table 3
Comparison results between the reservoir operation simulation and historical reservoir operation in two wet years (2005, 2013).

Data type	2005[d]	2005-H[e]	2013[d]	2013-H[e]
Total reservoir inflow (MCM)	1504	1504	1031	1504
IRS[a] (MCM)	161	148	161	165
HPO[b] (10^6 kWh)	140	65	137	59
FRS[c] (MCM)	192	171	201	199

[a] Initial reservoir storage (161 MCM) in October, which was set at a water level of 240 m for simulation purpose.
[b] Hydropower output during typhoon seasons.
[c] Final reservoir storage during non-typhoon seasons.
[d] Reservoir operation based on the NSGA-II for typhoon seasons (July–September) and M-5 rules curves for non-typhoon seasons (October–next June).
[e] Historical reservoir operation.

reservoir operation for mitigating water deficit conditions, especially for drought years. The benefit of hydropower output was 66.67 USD/MW·h based on current hydropower price released from the Shihmen Reservoir and Taiwan Power Company.

For evaluating the contribution of irrigation ponds to reservoir water supply during non-typhoon seasons, we next investigated the effort of integrating the reservoir with irrigation ponds in selected years during 2002 and 2015, where the initial reservoir storages (in October) was set as the optimized final reservoir storages (in September) in typhoon seasons while the initial storage of the virtual reservoir (the union of 745 ponds) was assumed to reach a total capacity of 62.38 million m^3. Fig. 7(a) and (b) show the agricultural and public water shortage rates, with (yellow bar in Fig. 7(a), red bar in Fig. 7(b)) and without (blue bar in Fig. 7) the incorporation of irrigation ponds into reservoir operation for non-typhoon seasons in selected years, respectively. Apparently, both agricultural and public water shortage rates significantly decreased in all the selected years as irrigation ponds being fused with reservoir operation, where the shortage rates were reduced by 22.2% and 23.7% in average for agricultural and public sectors, respectively. The results clearly presented the significant distinction between the inclusion and exclusion of irrigation ponds during reservoir operation. Consequently, if irrigation ponds could be fulfilled at the end of typhoon seasons (September), the Shihmen Reservoir combined with irrigation ponds could be capable of ameliorating unsatisfied water demands such that both agricultural and public water deficits could be mitigated in the future.

Table 4 shows the synergistic benefits of the WFE Nexus based on the optimal results given by the integration of short- and long-term reservoir operation coupled with irrigation ponds in two wet years (2005 and 2013).

The improvement values were the comparative results of the optimal reservoir operations with historical ones. The results indicated that in the water supply sector, the improvement rates in water deficit were 10% in 2015 and 1% in 2013 while in the food production sector, the improvement rates were 42% in 2005 and 47% in 2013. In the energy production sector, the hydropower benefits were 9.33 million in USD in 2005 and 9.13 million in USD in 2013, where the corresponding improvement rates were 115% and 132%, respectively. Consequently, the proposed scheme was demonstrated to improve the effectiveness and benefits of the WFE Nexus. That is to say, the synergistic benefits of the WFE Nexus obtained from our proposed mathodology could be much more promoted. as compared with those of historical operations

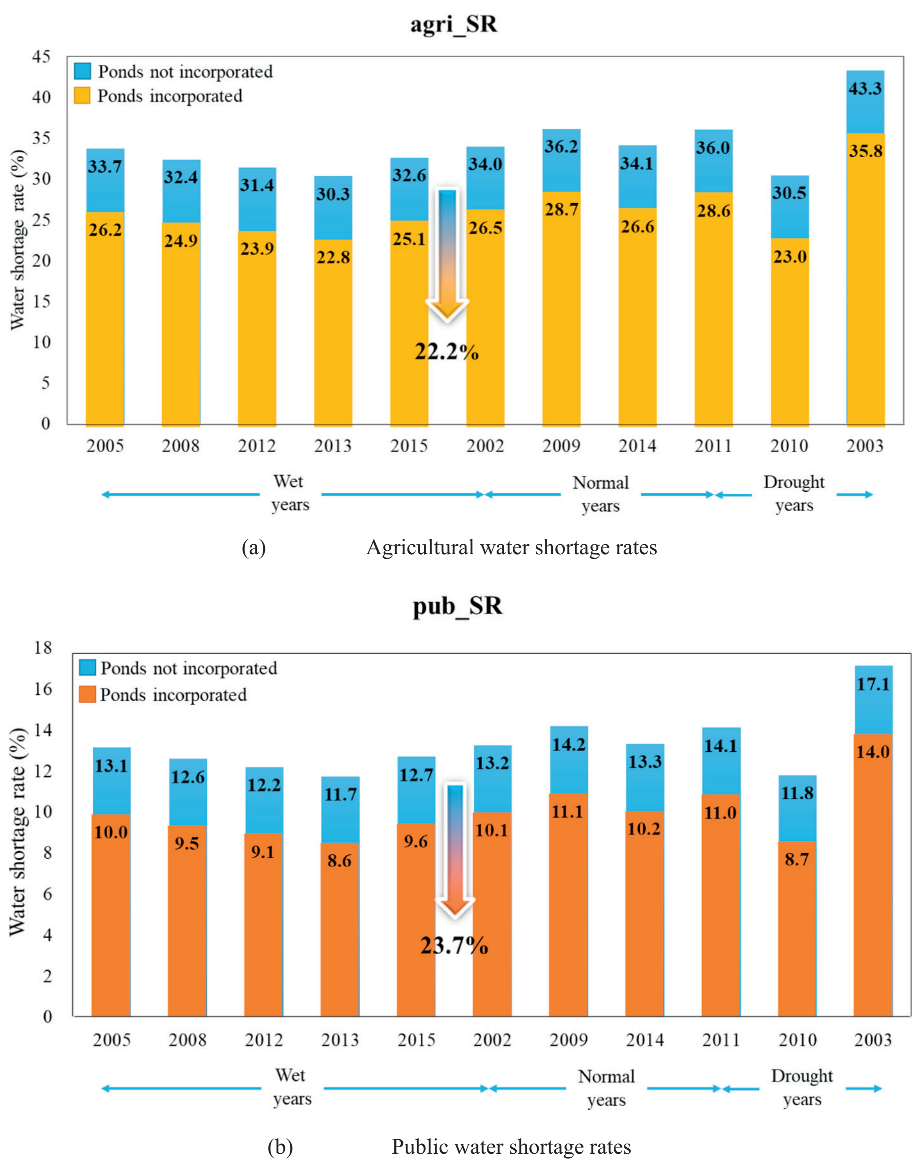

Fig. 7. Improvement results of agricultural and public water shortage rates with respect to the incorporation of irrigation ponds into reservoir operation during non-typhoon seasons, respectively.

Table 4
Synergistic benefits of WFE Nexus obtained from the optimal results given by the integration of short- and long-term reservoir operation coupled with irrigation ponds in two wet years, where historical reservoir operations were the benchmarks.

Nexus	IRS[a] = 161 (MCM)	2005	2013
Water	AWSR[b] (%)	16 (**10%**[e])	16 (**1%**)
Food	TFP[c] (10^6 kg)	65 (**42%**)	69 (**47%**)
Energy	HPB[d] (10^6 in USD)	9.33 (**115%**)	9.13 (**132%**)

[a] Initial reservoir storage in October.
[b] Average water shortage rate (agricultural and public) over all ten-day periods during non-typhoon seasons.
[c] Total food production per year (including vegetables and fruits).
[d] Hydropower benefits during typhoon seasons.
[e] Values in bold represent improvement rates.

implemented solely by M-5 rules curves. We noticed that several achievements were made by the proposed optimal reservoir opertions in 2013: the hydropower benefits surpassed 132% than the historical operations; the water shortage rates for both agricultural and public sectors were mitigated because of the joint operation with irrigtion ponds; and food production increased 47% owing to less agricultural water shortage.

We further investigated the reliability and effectiveness of the proposed methodology. Fig. 8 shows the improvement of hydropower benefits and average water shortage rate (AWSR) obtained from the proposed scheme under four scenarios (A: hydropower generation solely; B: hydropower generation favorable; C: water supply favorable; and D: water supply solely) for three hydrological types in ten selected years (i.e., 5 wet years, 3 normal years and 2 drought years) during 2002 and 2015, respectively, as compared to those of historical operations. Fig. 8(a) clearly indicated that hydropower benefits could be significantly improved for all the three hydrological-type years under Scenarios A and B but would decreased under Scenario D. On the other hand, the AWSR would largely mitigated in drought and normal years under Scenarios A and B (for instance, 75% for normal years and over 85% for drought years under Scenario A) while the AWSR could be mitigated in all three hydrological-type years under Scenario D. We also noticed that the AWSR remained the same in the wet years for all the four scenarios. This analysis suggested that there was a great potential (capability) for increasing the hydropower benefits without spending extra cost on the AWSR in wet years (even in normal years) if the proposed methodology could be implemented.

5. Conclusion

Sustainable urban development depends on a robust supply of water, food and energy; nevertheless, the complex linkages and multi-functions of water-food-energy resources pose a great challenge to synergistically optimize the benefits of the WFE Nexus. Reservoirs can enhance water availability, flood control, hydropower output as well as other services, and they play a key role in the WEF Nexus. This study proposed a holistic three-fold scheme that synergistically optimized the benefits of the WFE Nexus based on the short/long-term joint operation of a multi-objective reservoir and irrigation ponds. The Shihmen Reservoir coupled with 745 irrigation ponds (a backup for the reservoir) and its multiple users in northern Taiwan were selected as a case study. The historical reservoir operation based on M-5 rule curves was selected as a benchmark for comparison purpose.

The results showed that the short-term (daily scale) optimal reservoir operation obtained from the NSGA-II during typhoon seasons could improve hydropower output and raised the final reservoir storage, in comparison to historical reservoir operation. Moreover, the combination of the reservoir operation simulated by the M-5 rule curves coupled with irrigation ponds could decrease the long-term (ten-day scale) water shortage rates in both agricultural and public sectors during non-typhoon seasons. That is, integrating the reservoir with irrigation ponds could improve long-term water supply benefits. The integration of short/long term optimal reservoir operation and irrigation ponds not only could improve energy production but also enhance water supply and food production from a year-round perspective. Thus, the proposed short/long-term joint reservoir operation methodology could be implemented as one of the robust solutions to improving the synergistic benefits of the WFE Nexus. Our results demonstrated that the proposed methodology could build a synergistic WFE reallocation scheme in northern Taiwan, which would deliver feasible and socially acceptable governance strategies on the WFE Nexus to assist decision-makers and stakeholders in WFE resource management. These findings lead sustainable urban development plans that cover short-term and long-term policy implications.

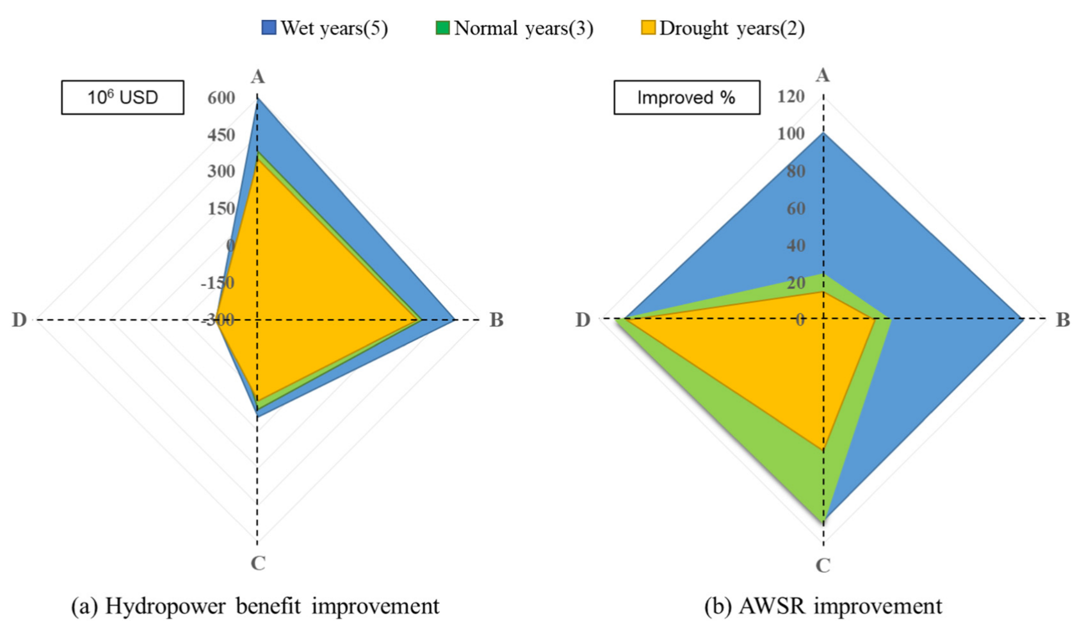

Fig. 8. Improvement comparison of (a) hydropower benefit and (b) average water shortage rate (AWSR) obtained from the proposed scheme under scenarios A–D in selected wet, normal and drought years during 2002 and 2015, respectively, as compared to those of historical reservoir operations. A: Optimal solutions fully satisfying the water demand of hydropower generation B: Compromised solutions for wet years C: Compromised solutions for normal years D: Optimal solutions fully satisfying water supply reliability (compromised solution for drought years).

Acknowledgements

This study was financially supported by the Ministry of Science and Technology, Taiwan, ROC (Grant Numbers 105-2627-M-002-035, 106-2627-M-002-025 and 105-2811-B-002-151).

References

Ahmad, A., El-Shafie, A., Razali, S.F.M., Mohamad, Z.S., 2014. Reservoir optimization in water resources: a review. Water Resour. Manag. 28 (11), 3391–3405.
Ali, B., Kumar, A., 2017. Development of life cycle water footprints for oil sands-based transportation fuel production. Energy 131 (10), 41–49.
Allan, T., Keulertz, M., Woertz, E., 2015. The water–food–energy nexus: an introduction to nexus concepts and some conceptual and operational problems. Int. J. Water Resour. Dev. 31 (3), 301–331.
Al-Saidi, M., Elagib, N.A., 2017. Towards understanding the integrative approach of the water, energy and food nexus. Sci. Total Environ. 574, 1131–1139.
Bai, T., Chang, J.X., Chang, F.J., Huang, Q., Wang, Y.M., Chen, G.S., 2015. Synergistic gains from the multi-objective optimal operation of cascade reservoirs in the Upper Yellow River basin. J. Hydrol. 523 (8), 758–767.
Barik, B., Ghosh, S., Sahana, A.S., Pathak, A., Sekhar, M., 2017. Water-food-energy nexus with changing agricultural scenarios in India during recent decades. Hydrol. Earth Syst. Sci. 21 (9), 3041–3060.
Bieber, N., Ker, J.H., Wang, X., Triantafyllidis, C., van Dam, K.H., Koppelaar, R.H.E.M., Shah, N., 2018. Sustainable planning of the Energy-Water-Food nexus using decision making tools. Energy Policy 113, 584–607.
Castelletti, A., Pianosi, F., Quach, X., Soncini-Sessa, R., 2012. Assessing water reservoirs management and development in Northern Vietnam. Hydrol. Earth Syst. Sci. 16 (6), 189–199.
Chang, L.C., 2008. Guiding rational reservoir flood operation using penalty-type genetic algorithm. J. Hydrol. 354 (1–4), 65–74.
Chang, L.C., Chang, F.J., 2009. Multi-objective evolutionary algorithm for operating parallel reservoir system. J. Hydrol. 377 (1), 12–20.
Chang, Y., Li, G., Yao, Y., Zhang, L., Yu, C., 2016a. Quantifying the Water-Energy-Food Nexus: current status and trends. Energies 9 (2), 65.
Chang, F.J., Wang, Y.C., Tsai, W.P., 2016b. Modelling intelligent water resources allocation for multi-users. Water Resour. Manag. 30 (4), 1395–1413.
Chini, C.M., Konar, M., Stillwell, A.S., 2017. Direct and indirect urban water footprints of the United States. Water Resour.Res. 53 (1), 316–327.
Chou, N.F., Wu, C.W., 2015. Stage-wise optimizing operating rules for flood control in a multi-purpose reservoir. J. Hydrol. 521 (5), 245–260.
Chu, J., Zhang, C., Fu, G., Li, Y., Zhou, H., 2015. Improving multi-objective reservoir operation optimization with sensitivity-informed dimension reduction. Hydrol. Earth Syst. Sci. 19 (1), 3557–3570.
Cosgrove, W.J., Loucks, D.P., 2015. Water management: current and future challenges and research directions. Water Resour. Res. 51 (6), 4823–4839.
De, C.M.D., Scanlon, B.R., Zhang, Z., Wendland, E., Yin, L., 2016. Reservoir storage and hydrologic responses to droughts in the Paraná River basin, south-eastern Brazil. Hydrol. Earth Syst. Sci. 20 (11), 4673.
Deb, K., Pratap, A., Agarwal, S., Meyarivan, T., 2000. A fast elitist non-dominated sorting genetic algorithm for multi-objective: NSGA-II. Proceedings of the Parallel Problem Solving From Nature VI Conference, pp. 846–858.
Deb, K., Pratap, A., Agarwal, S., Meyarivan, T., 2002. A fast and elitist multi-objective genetic algorithm: NSGA-II. IEEE Trans. Evol. Comput. 6 (2), 182–197.
El-Gafy, I.K., 2014. System dynamic model for crop production, water footprint, and virtual water nexus. Water Resour. Manag. 28 (13), 4467–4490.
Feng, M., Liu, P., Li, Z., Zhang, J., Liu, D., Xiong, L., 2016. Modeling the nexus across water supply, power generation and environment systems using the system dynamics approach: Hehuang Region, China. J. Hydrol. 543 (11), 344–359.
Garcia, D.J., You, F., 2016. The water-energy-food nexus and process systems engineering: a new focus. Comput. Chem. Eng. 91 (4), 49–67.
Haghighi, A., Asl, A.Z., 2014. Uncertainty analysis of water supply networks using the fuzzy set theory and NSGA-II. Eng. Appl. Artif. Intell. 32 (3), 270–282.
Hoekstra, A.Y., 2017. Water footprint assessment: evolvement of a new research field. Water Resour. Manag. 31 (14), 1–21.
Hsu, N.S., Huang, C.L., Wei, C.C., 2015. Multi-phase intelligent decision model for reservoir real-time flood control during typhoons. J. Hydrol. 522 (6), 11–34.
Hurford, A.P., Harou, J.J., 2014. Balancing ecosystem services with energy and food security - assessing trade-offs from reservoir operation and irrigation investments in Kenya's Tana Basin. Hydrol. Earth Syst. Sci. 18 (4), 3259–3277.
Jalilov, S.M., Keskinen, M., Varis, O., Amer, S., Ward, F.A., 2016. Managing the water-energy-food nexus: gains and losses from new water development in Amu Darya river basin. J. Hydrol. 539 (7), 648–661.
Machell, J., Prior, K., Allan, R., Andresen, J.M., 2015. The water energy food nexus-challenges and emerging solutions. Environ. Sci.: Water Res. Technol. 1 (1), 15–16.
Miller, L., Carriveau, R., 2017. Balancing the carbon and water footprints of the Ontario energy mix. Energy 125 (3), 562–568.
Owen, A.E., Scott, K., Barrett, J., 2018. Identifying critical supply chains and final products: an input-output approach to exploring the energy-water-food nexus. Appl. Energy 201, 632–642.
Pereira, L.S., 2017. Water, agriculture and food: challenges and issues. Water Resour. Manag. 31 (5), 2985–2997.
Ramos, H.M., Teyssier, C., López-Jiménez, P.A., 2013. Optimization of retention ponds to improve the drainage system elasticity for water-energy nexus. Water Resour. Manag. 27 (8), 2889–2898.
Rasul, G., Sharma, B., 2016. The nexus approach to water–energy–food security: an option for adaptation to climate change. Clim. Pol. 16 (6), 682–702.
Ringler, C., Bhaduri, A., Lawford, R., 2013. The nexus across water, energy, land and food (WELF): potential for improved resource use efficiency? Curr. Opin. Environ. Sustain. 5 (6), 617–624.
Scanlon, B.R., Ruddell, B.L., Reed, P.M., Hook, R.I., Zheng, C., Tidwell, V.C., Siebert, S., 2017. The food-energy-water nexus: transforming science for society. Water Resour. Res. 53 (5), 3550–3556.
Smajgl, A., Ward, J., Pluschke, L., 2016. The water-food-energy Nexus-realising a new paradigm. J. Hydrol. 533 (5), 533–540.
Tabari, M.M.R., Soltani, J., 2013. Multi-objective optimal model for conjunctive use management using SGAs and NSGA-II models. Water Resour. Manag. 27 (1), 37–53.
Tarroja, B., AghaKouchak, A., Sobhani, R., Feldman, D., Samuelsen, S., 2014. Evaluating options for balancing the water-electricity Nexus in California: part 1 – securing water availability. Sci. Total Environ. 293-594, 610–617.
Tsai, W.P., Chang, F.J., Chang, L.C., Herricks, E.E., 2015. AI techniques for optimizing multi-objective reservoir operation upon human and riverine ecosystem demands. J. Hydrol. 530 (11), 634–644.
Vilanova, M.R.N., Balestieri, J.A.P., 2015. Exploring the water-energy nexus in Brazil: the electricity use for water supply. Energy 85 (3), 415–432.
Vörösmarty, C.J., McIntyre, P.B., Gessner, M.O., Dudgeon, D., Prusevich, A., Green, P., ... Davies, P.M., 2010. Global threats to human water security and river biodiversity. Nature 467 (7315):555–561. https://doi.org/10.1038/nature09440.
Weitz, N., Strambo, C., Kemp-Benedict, E., Nilsson, M., 2017. Closing the governance gaps in the water-energy-food nexus: insights from integrative governance. Glob. Environ. Chang. 45, 165–173.
Wichelns, D., 2017. The water-energy-food nexus: is the increasing attention warranted, from either a research or policy perspective? Environ. Sci. Pol. 69, 113–123.
Zhang, X., Vesselinov, V.V., 2017. Integrated modeling approach for optimal management of water, energy and food security nexus. Adv. Water Resour. 101 (3), 1–10.
Zhou, Y., Guo, S., Xu, C.Y., Liu, D., Chen, L., Ye, Y., 2015. Integrated optimal allocation model for complex adaptive system of water resources management (I): methodologies. J. Hydrol. 531 (11), 964–976.